Feature Extraction and 3D Reconstruction of Nomarski DIC Microscope Images Using Local Energy and Neural Net Techniques

Matthew Kyan*[a], Ling Guan[a], Matthew Arnison[b], Carol Cogswell[b]

[a]Dept. of Electrical Engineering, University of Sydney, NSW 2006, Australia

[b]School of Physics, University of Sydney, NSW 2006, Australia

ABSTRACT

The Nomarski differential interference contrast (DIC) mode is commonly used for imaging translucent biological specimens and it exhibits several major advantages over other phase contrast techniques, including a boost in high spatial frequencies in the region of focus. However, DIC images (unlike confocal) are limited by the presence of low spatial frequency blur and also by a differential shading gradient at feature boundaries, which make normal confocal visualisation techniques unsuitable for feature extraction or for 3D volume rendering of focus-series datasets.

To remedy this problem, we employ a neural network technique based on competitive learning, known as Kohonen's self-organising feature map (SOFM), to perform segmentation, using a collection of statistics (know as features) defining the image. Our past investigation showed that standard features such as the *localised mean* and *variance* of pixel intensities provided reasonable extraction of objects such asmitotic chromosomes, but surface detail was only moderately resolved. In this current work, *local energy* is investigated as an alternative image statistic based on phase congruency in the image. This, along with different combinations of other image statistics, is applied in a SOFM, producing 3D images exhibiting vast improvement in the level of detail and clearly isolating the chromosomes from the background.

Keywords: differential interference contrast, DIC, feature extraction, feature space, image segmentation, self organising feature map, SOFM, phase congruency, local energy, Morlet wavelet

1. INTRODUCTION

Confocal microscopy is widely becoming a popular method for imaging specimens across 3D volumes, the results of which subsequently reflect structural and surface detail not visible in standard 2D projections[1]. The confocal configuration (i.e. point-like illumination and a detector with a pinhole mask) demonstrates increased ability for *optical sectioning* (improved depth resolution) over conventional methods (i.e. using a large-area-detector), thus making it ideal for obtaining highly resolved image slices across the specimen volume, which can then be recombined to form a 3D image representation.

Confocal transmission differential interference contrast is a mode that essentially images changes in the refractive index of the specimen, thus it is suited to the imaging of translucent subjects, such as chromosomes[2]. A problem arises however in that the DIC image shows a differential *bas-relief* effect, depicting highlights for positive phase gradients in the specimen, shadows for negative gradients and grey for regions of zero phase gradient (or a level surface). As a result, it becomes difficult to distinguish the level surfaces on the chromosomes from the background, prompting the need for removing the differential effect and reconstructing the original image. While reconstruction alone does offer a specimen that can be viewed in 3D, further image segmentation can resolve greater surface detail within the objects themselves than can be obtained through a simple background removal.

* Correspondence: email: m.kyan@physics.usyd.edu.au

Part of the SPIE Conference on Three-Dimensional and Multidimensional Microscopy: Image Acquisition and Processing VI • San Jose, California • January 1999
SPIE Vol. 3605 • 0277-786X/99/$10.00

Image segmentation is the process of subdividing or categorising an image into its different constituent parts. This may be simply to separate the objects within an image from the background itself, or may extend further, to the separation of different types of surfaces existing within the image.
Surface characteristics can be defined in terms of the concept of feature space. This simply refers to the vectorial representation of a group of image statistics such as intensity, localised mean or variance of a particular pixel location in the image. The number of features used to define that pixel corresponds to the number of dimensions defining its vector in feature space.

Kohonen's SOFM algorithm provides the final mechanism for analysis, categorising the various features (defined in feature space) of the image. It breaks the image up into clusters representing regions of similarity. These regions then reflect a surface topology, highlighting important details of the objects within the specimen. Volume visualisation provided through the software package *VoxelView*, can then be implemented in order to display the segmented data. Specifically, the 3D display is such that pixels or voxels (equivalent 3D picture elements) belonging to certain surface categories are made transparent, revealing the remaining chromosome structures.

2. IMAGE RECONSTRUCTION

The first stage in processing the DIC image data is to remove the differential *bas-relief* effect present in the image (Figure 1a). The technique used is based on spatial frequency analysis, and is known as the Hilbert transform (developed by Oppenheim and Schafer)[3].

In the real space domain, differentiation corresponds to a multiplication by the spatial frequency, whereas integration corresponds to division. Straight integration alone induces a division process that attenuates higher frequency components, often resulting in a blurred result. The Hilbert transform differs in its ability to maintain the relative balance of frequency components in the image. It achieves this by keeping all positive frequency components and reversing the negative frequency components (Figure 1b). This makes the image symmetric, removing the *bas-relief* effect.

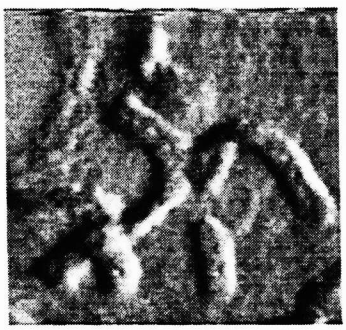

(a) One of the original 2D transmission DIC images of orchid chromosomes showing *bas-relief* (differential shading gradient)

(b) Hilbert transform of the DIC image shown in Figure 1a. The differential shading is removed, providing an initial stage in image reconstruction.

Figure 1: Image Reconstruction

3. IMAGE SEGMENTATION USING SOFM

Kohonen's self-organising map algorithm can be visualised in terms of the structure shown in Figure 2. Input feature vectors are applied to the input node of the SOFM one at a time, each imparting information to the neural map about a particular characteristic in the image. Each neuron in the map has a feature vector of its own, initially randomly oriented in feature space. Over time these neurons learn from the input vectors, according to a competitive learning algorithm, gradually *tuning* themselves to a particular orientation in feature space. The final orientations of the neurons then represent particular feature categories into which the individual image pixels (denoted by the input feature vectors) can be grouped. The final categorisation of pixels reflects a segmentation of the original image.

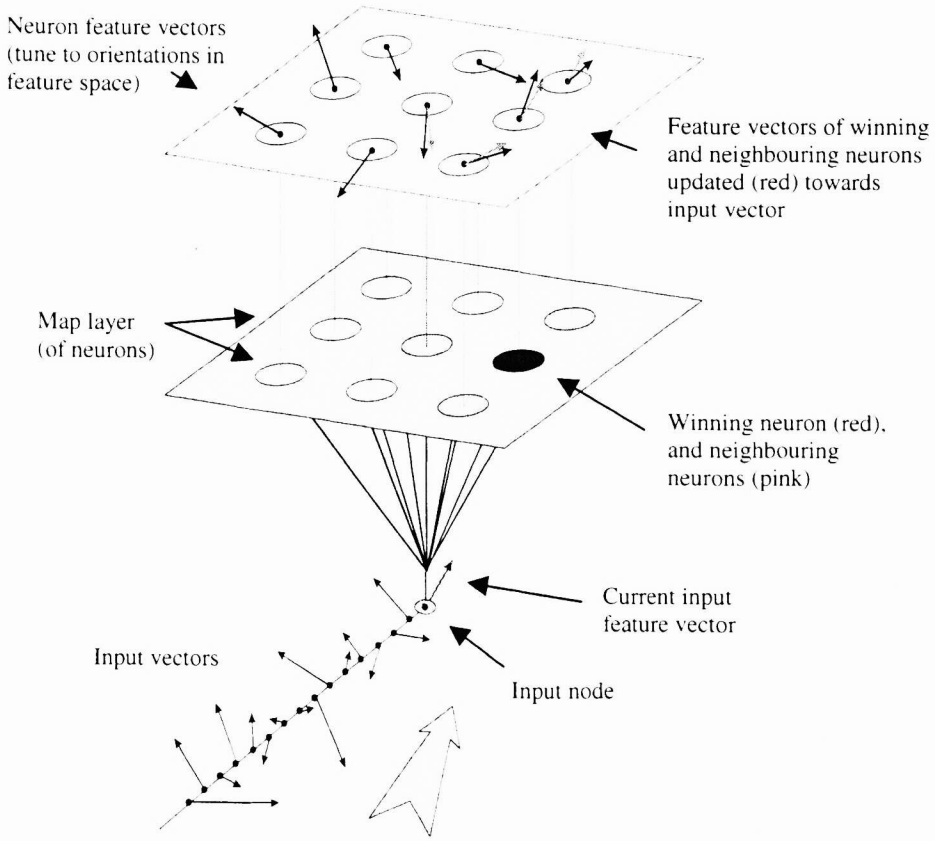

Figure 2: Kohonen's Self Organising Feature Map algorithm

When each input vector is applied to the network, a single neuron known as the *winning* neuron is activated. This neuron is the one with a feature vector closest to the input vector. The *winning* neuron is found by calculating the minimum euclidean distance of all the neurons from the input vector as follows, where $m_i(t)$ is the feature vector of neuron i, $x(t)$ is the current input vector, and c is the winning neuron :

$$\|x(t) - m_c(t)\| = \min_i \{\|x(t) - m_i(t)\|\} = \min_i \left\{ \sqrt{\sum_{j=1}^{n} (x_j(t) - m_{i,j}(t))^2} \right\} \quad (1)$$

The winning neuron and its neighbouring neurons, each learn information by updating their orientations toward the input vector by some proportion. The proportion is highest for the winning neuron, reducing somewhat for the surrounding neurons, depending on how close they are to the winning neuron. Closer neurons are updated more dramatically thus learn more information from the input. The learning process is iterative, converging over time:

$$m_i(t+1) = m_i(t) + \alpha(t) h_{c_i}(t)[x(t) - m_i(t)] \tag{2}$$

Where $h_{ci}(t)$ is a neighbourhood smoothing function modelled on a gaussian, and $\alpha(t)$ describes the learning rate of the neural net, which decays to zero over time, forcing convergence[4].

4. LOCAL ENERGY DETECTION

The concept of local energy (LE) or phase congruency (PC) is based on physiological evidence[5] suggesting that the human visual system responds strongly to points in an image where phase information is highly ordered. As such the local energy model searches for patterns of *order* in the phase component of the Fourier transform of the image. This essentially translates to the idea that humans tend to perceive features in an image at points of maximal phase congruency.

Phase congruency, defined by Morrone and Owens[6], is, of itself, a difficult quantity to calculate. Subsequently, it was found by Venkatesh and Owens[7] that peaks in the PC function correspond to peaks in a popular calculation used in biological vision, namely the local energy E(x):

$$E(x) = \sqrt{F^2(x) + H^2(x)} \tag{3}$$

$$E(x) = PC(x) \sum_n A_n \tag{4}$$

Where F(x) is the one dimensional luminance profile and H(x) is the Hilbert transform of F(x).

The preferred method of calculating local energy is via the wavelet transform[8]. This method uses a bank of filters created from rescalings of one type of wave shape, to analyse the signal. Each scaling is designed to 'pick out' particular frequencies of the signal being analysed[9]. Morlet wavelets are used for this purpose. They are based on complex Gabor functions: cosine waves (even) and sine waves (odd), each modulated by a gaussian.

Sets of real and imaginary wavelet pairs (each tuned to a particular frequency) are combined over a range of frequencies, *Freq*, forming the filter bank. Each pair acts separately on the image (summing over the frequency range to produce the separate components of local energy, F(x) and H(x), where I(x) denotes the image):

$$F(x) = \sum_{f=Freq} I(x) \otimes M_f^{even}(x) \tag{5}$$

$$H(x) = \sum_{f=Freq} I(x) \otimes M_f^{odd}(x) \tag{6}$$

where M_f^{even} and M_f^{odd} form the Morlet wavelets at a particular frequency f.

The even and odd morlet wavelets used are defined respectively as:

$$M_{f,\hat{v}(x)}^{even} = \frac{1}{\left(\sqrt{2\pi}\sigma\right)^3} e^{-\|x\|^2/2\sigma^2} \omega \cos\left(\omega \hat{v}^T \cdot x\right) \tag{7}$$

$$M_{f,\hat{v}(x)}^{odd} = \frac{1}{\left(\sqrt{2\pi}\sigma\right)^3} e^{-\|x\|^2/2\sigma^2} \omega \sin\left(\omega \hat{v}^T \cdot x\right) \tag{8}$$

where σ is the width of the wavelet filter, ω is the frequency ($2\pi f$), and $\hat{v}$ is the direction in which the wavelet is oriented when extended to higher dimension signals such as 2D or 3D images.

When extended to calculation in 3D, the wavelet filters exhibit an imposed orientation (defined in equations 7 and 8). Thus it becomes necessary to calculate local energy using banks of Morlet filters oriented in 3D space. Each oriented filter contributes to a portion of the final local energy distribution, summing over the 3D image volume.

5. RESULTS

Primary simulations were conducted on test cases of an 18 slice dataset for the purpose of examining the effects on the segmented result due to different combinations of input features. The sets of features (each 3-fold) used in each test case were:

Case 1: {pixel intensity (PI), localised mean (M), localised variance (V)}
Case 2: {PI, M, local energy (LE)}
Case 3: {PI, LE, V}
Case 4: {LE, localised mean of LE, localised variance of LE}

Local energy (LE) calculations were made on the hilbert transformed image data, over a series of 20 orientations in 3D space.

The test cases were applied to various sized SOFM maps, including 3x3, 4x4, 5x5: corresponding to 9, 16 & 25 neurons or categories of feature classification respectively. The resultant volume visualisations are presented in Figure 3(a-d) for each test case, as applied to a 4x4 SOFM used to segment an 18 slice image dataset of an orchid root tip specimen.

In Figure 3(a) and (b), which incorporate the mean of the original pixel intensities, the segmentation tends to blur or reveal somewhat coagulated chromosome bodies, with Figure 3(b), (using local energy) revealing slightly more surface detail. Figure 3(d), using only LE based statistics, produced an extremely highly detailed result, showing very dramatic (perhaps exaggerated) variations across the chromosome surfaces. This result reflects the hypersensitivity of the local energy function to different feature profiles in the image. Finally, Figure 3(c), using local energy and variance, depicts a dramatic improvement in clarity of the fine structure of the chromosomes, to the point where the two components making up a chromosome (known as *sister chromatids*) are visibly twisted or coiled together, in some places bunched up – a property consistent with the stage of cell mitosis in which the chromosomes were imaged.

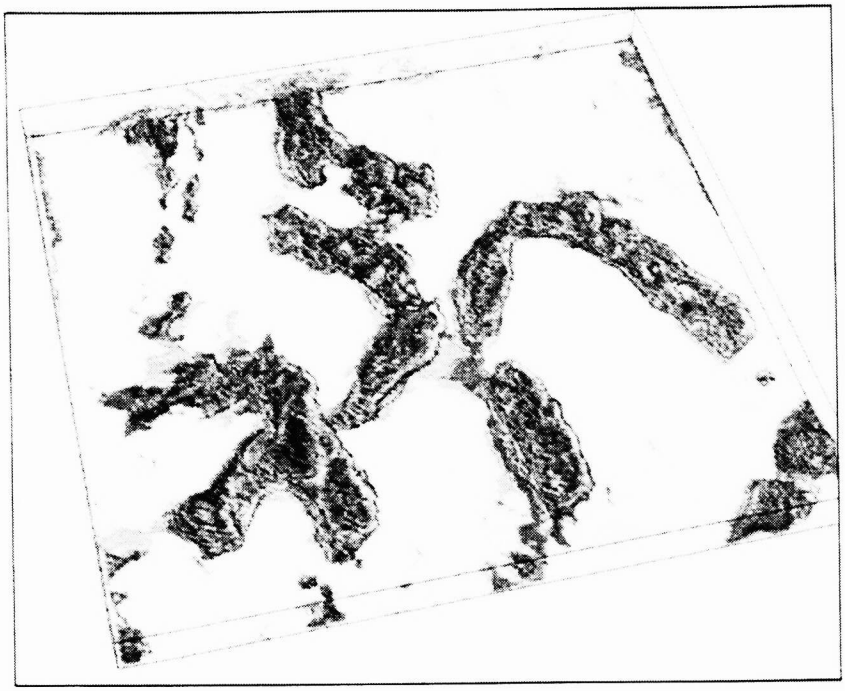

Figure 3a: **Case 1 –** Volume visualisation of an 18 slice data set of orchid root tip chromosomes after segmentation using a 4x4 SOFM and case 1 image statistics

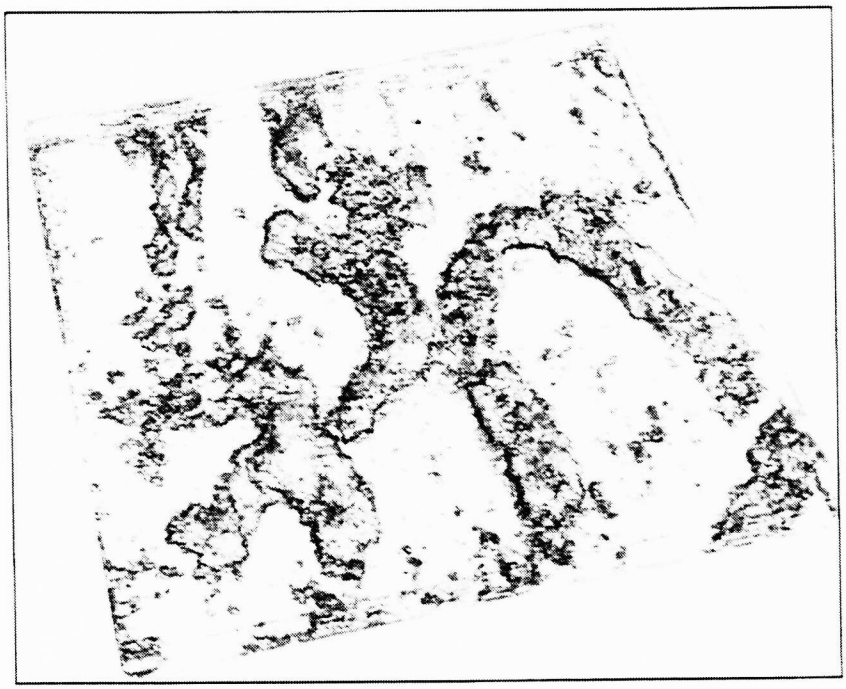

Figure 3b: **Case 2 –** Volume visualisation of an 18 slice data set of orchid root tip chromosomes after segmentation using a 4x4 SOFM and case 2 image statistics

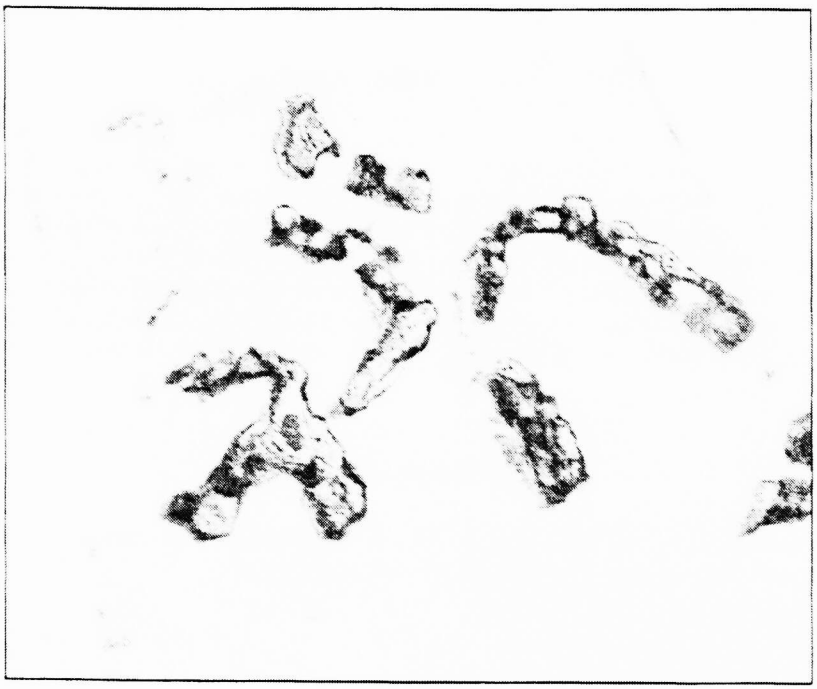

Figure 3c: **Case 3-** Volume visualisation of an 18 slice data set of orchid root tip chromosomes after segmentation using a 4x4 SOFM and case 3 image statistics

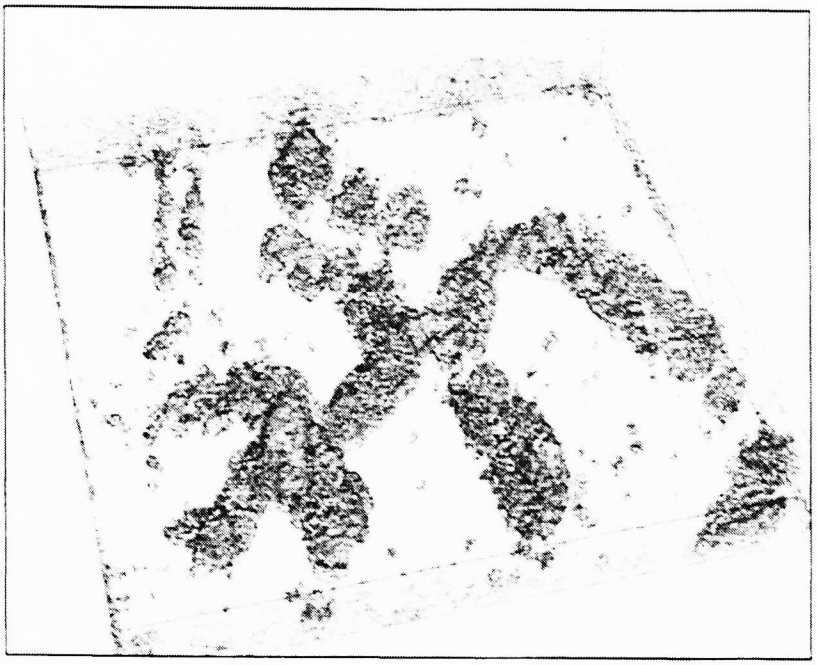

Figure 3d: **Case 4-** Volume visualisation of an 18 slice data set of orchid root tip chromosomes after segmentation using a 4x4 SOFM and case 4 image statistics

6. CONCLUSIONS

The use of the confocal microscope to image translucent specimens such as chromosomes, allows for increased optical sectioning across a specimen volume, aiding in the formation of 3D image data. The DIC mode used to produce the image slices, however, requires further image processing in order that the objects within the specimen volume can be extracted from the image background. Kohonen's self organising feature map is a neural network approach to segmenting the chromosomes within the image volume, resulting in adequate extraction of the chromosome bodies, as well as resolving surface detail of their structure. Local energy has been explored as a possible feature to be used in directing the SOFM during segmentation, along with other standard features such as original, mean and variance of pixel intensities. Local energy has shown to be an extremely effective feature for resolving surface details of chromosomes from confocal DIC images beyond levels achieved in the past. Visualisation of chromosome images produced in this fashion is possible, greatly enhancing the ability for biologists to observe, in 3D, the intricate nature of plant chromosomes.

ACKNOWLEDGEMENTS

Special thanks to the Physical Optics dept, University of Sydney, as well as to the staff of Sydney Vislab[†] for technical assistance and resources offered for use in the visualisation of resultant datasets

REFERENCES

1. C.J.Cogswell, K.G.Larkin, M.R.Arnison and J.W.O'Byrne. "3D Fourier analysis methods for digital processing and 3D visualisation of confocal transmission images". *SPIE* **2412**, 230-235 (1995).

2. C.J.Cogswell and C.J.R.Steppard. "Confocal differential interference contrast (DIC) microscopy: including a theoretical analysis of conventional and confocal DIC imaging". *Journal of Microscopy*, **165** (1):81-101 (1992)

3. A.Oppenheim and R.Schafer. *Discrete-time signal processing*, New Jersey, Prentice Hall (1989).

4. S.Haykin. *Neural Networks a comprehensive foundation.* New York, Macmillan College (1994).

5. M. C.Morrone and D.C.Burr. "Feature detection in human vision: A phase-dependent energy model". *Proceedings of the Royal Society of London B*, **235**:221-245 (1988).

6. M.C.Morrone and R.A.Owens. "Feature detection from local energy". *Patt. Recog. Lett.* **6**:303-313 (1987).

7. S.Venkatesh and R.A.Owens. "An energy feature detection scheme". IEEE Int. Conf. On image processing, Singapore, 553-557. (1989)

8. J.Morlet, G.Avens, E.Fourgeau and D.Giard. "Wave propagation and sampling theory – Part II: Sampling theory and complex waves". *Geophysics* **47** (2):222-236 (1982)

9. C.Pudney, M.Robins, B.Robbins and P.Kovesi. "Surface detection in 3D confocal microscope images via local energy and ridge tracing". *Journal of Computer-Assisted Microscopy,* **8** (1):5-20 (1996)

[†] http://www.vislab.usyd.edu.au/